Mineralogy and Petrology (2003) 78: 255–268
DOI 10.1007/s00710-002-0236-x

Mineralogy and Petrology

Printed in Austria

An electron microscopy study of deformation microstructures in granitic mylonites from southwestern Sweden, with special emphasis on the micas

A. Ooteman, E. A. Ferrow, and **A. Lindh**

Mineralogy and Petrology, Department of Geology, Lund University, Lund, Sweden

Received October 15, 2001; revised version accepted December 25, 2002
Published online June 2, 2003;
Editorial handling: C. Ballhaus

Summary

The lithology, age, geological setting, structural and metamorphic history of the granitic mylonites from the Mylonite Zone (MZ) in southwestern Sweden have been studied extensively. The deformation history, growth of microstructures, intensity of deformation, changes in mineral compositions, and pressure-temperature conditions of deformation have, however, not been addressed. In this study, powder X-ray diffraction, optical microscopy, electron microprobe analysis and transmission electron microscopy of micas, chlorite, and plagioclase are combined to understand the physical and textural changes experienced by the rocks during mylonitization. It is shown that the occurrence of foliated micas in shear bands, recrystallization of quartz and biotite, and undulatory extinction in quartz grains were not uniform throughout the samples studied. Occurrence of dislocations and low-angle grain boundaries confirm that deformation occurred largely by glide dislocations. The low-angle grain boundaries observed are formed by the re-arrangement of these dislocations during grain size reduction processes. The micas show a high degree of spatial stacking order, but spatial stacking disorder in micas and chlorites has also been found.

Ordered stacking faults are formed during low strain while disordered stacking faults are formed under high strain conditions. Occurrence of both ordered and disordered stacking faults indicates that the intensity of deformation was not uniform through the entire MZ. Moreover, the chemical composition of plagioclase shows that the exsolution lamellae observed with optical and electron microscopy are due to Ca-subsolidus reactions during low temperature deformation. Several substitution reactions occurring in the micas indicate that deformation took place between 0.3 and 0.4 GPa, at a temperature higher than 500 °C.

Introduction

A mylonite zone can be considered as a ductile shear zone, situated at a deeper crustal level (*Carreras* et al., 1980). Characteristic features of mylonites include (1) grain-size, reduction, (2) the occurrence in relatively narrow, planar zones up to several tens of kilometers in length, and (3) enhanced foliation and/or lineation. Mylonite zones are attractive for studies of ductile deformation of crustal rocks.

Some parts of the granitic mylonites from the Mylonite Zone in southwestern Sweden (MZ) belong to a lithological unit called the Micaceous Gneiss (*Lindh*, 1974, 1998). Mylonites are formed by grain refinement in a steady-state process caused by high strain rates. The process is ductile and produces a fine-grained foliated rock, usually much finer-grained than its protolith. The foliation is often crude but sometimes well developed. Mylonites are associated with ductile processes, during which deformation, dislocations, re-crystallization (grain size reduction), chemical substitutions, and exsolution lamellae occur in response to changes in temperature and pressure. The formation of shear bands in mylonites is typical for these rocks.

In this study, several samples of granitic mylonites, sharing almost identical pressure, temperature, and deformation histories, are examined with optical and Transmission Electron Microscopy (TEM). The purpose of this study is to (1) examine the deformation and growth microstructures, (2) monitor the changes in crystal chemistry of the phases, and (3) estimate the physical conditions (P, T) prevailing during mylonitization. Emphasis will be on microstructures of the micas to document dislocation structures, dislocation density, polytypism, and exsolution features. Microprobe analysis in combination with powder X-ray diffraction will be used to estimate pressure-temperature conditions under which the granitic mylonites formed.

Geological setting and sample description

The MZ in southwestern Sweden is a prominent arc-formed shear zone (Fig. 1). To the east of the zone is a 50 to 60 km wide belt of granitoid gneisses. These rocks are metamorphosed counterparts of the Transscandinavian Igneous Belt (TIB) intruded partly during the waning stage of the early Proterozoic Svecofennian orogeny and partly significantly later. The rocks to the west of the MZ are younger than the main part of the TIB intrusions but considerably older than the metamorphism; they have a long history of repeated granite intrusions. The age of the Zone is not very well constrained but lies between 900 and 1000 Ma (*Page*, 1996).

In the wider part of the MZ, the degree of deformation varies. The zone seems to consist of a series of anastomozing fault zones. Discrete, thinner shear zones striking north–south join the MZ from its northwestern side (*Lindh*, 1980a). Simultaneously, more strongly deformed rocks appear along the northwestern boundary of the zone, making its northern border less well-defined.

For the present investigation, samples from three localities are used. Two of these, S72 and S194, were taken from within the MZ. The third sample, S371, comes from a strongly deformed, hydrothermally overprinted gneissic band to the south of the zone (Fig. 1). All three samples contain abundant newly formed white mica. Earlier analysis of similar white micas from the MZ has revealed a fairly high celadonite component (*Lindh*, 1980b).

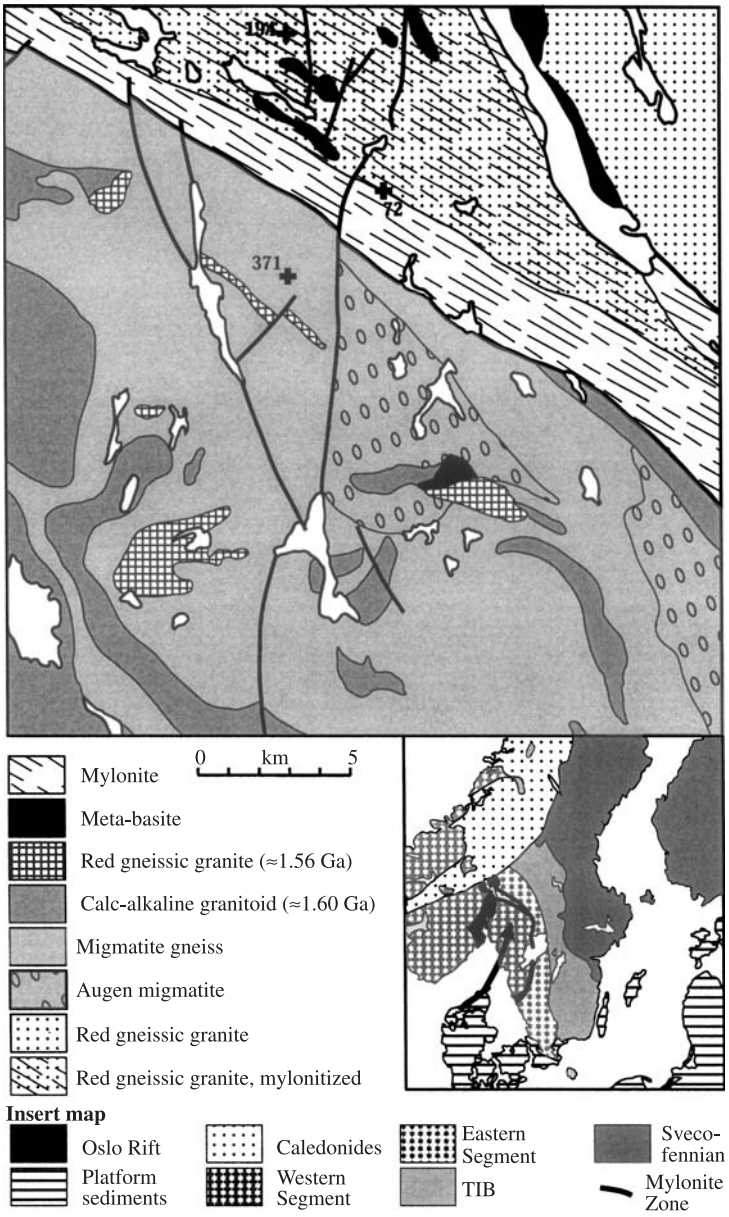

Fig. 1. Simplified geological map of the study area (after *Lundegårdh* et al., 1992). The Mylonite Zone (MZ) constitutes the border between the Eastern and Western Segments of SW Sweden. Samples are taken from both segments and from the boundary zone between them. The arrow in the key map shows the location of the larger-scale map. Lake Vänern is the large lake shown in the insert

Sample S72 is taken in the MZ close to the border between the southern and the northern blocks, probably a few meters inside the southern block. The area is strongly deformed and hydrothermally overprinted; consequently it is not possible to identify the protolith. Mylonite, which definitely belongs to the northern block, occurs approximately fifty meters to the north of the sampled locality.

Macroscopically, the rock is banded on a mm-, cm-, and dm-scale. The thinnest bands are almost monomineralic, whereas a lithological felsic-mafic contrast defines the thickest bands. The rock is foliated, with quartz bands defining the foliation. Porphyroclasts of feldspar are orientated in the foliation direction. They are strongly altered and contain minute irregular flakes of white mica. Albite twinning is discernible in some grains. White mica occurs in multi-grain bundles wrapped around the feldspar megacrysts. Small crystals of probable zircon occur inside these bundles. At another locality, larger similar bundles have been found to contain cores of relict kyanite.

Sample S194 is from rocks from the northern block of the MZ. In Fig. 1, the various granites making up the northern block have not been discriminated. The original rock is a strongly foliated granite gneiss with K-feldspar megacrysts. Much of the original feldspar is transformed into white mica. The unit can be followed along strike into rocks composed almost entirely of quartz and white mica, passing a transitional stage containing abundant epidote. Quartz grains and sub-grains, biotite, and white micas define the foliation, which sweeps around the K-feldspar megacrysts. These megacrysts are cracked and the cracks are filled with quartz. Quartz has also crystallized in pressure shadows. Clear, albite-twinned plagioclase crystals studded by small flakes of white mica are common. Optically zoned epidote and calcite occur in lesser amounts.

The third sample, S371, from the area south of the MZ, is different. It is a grey-coloured, veined, medium-grained gneiss, derived from a thin horizon of hydrothermally overprinted and deformed rocks. The rock complex is interpreted to be part of the oldest plutonic rocks of the area. White mica and biotite define the foliation. Most mica flakes closely follow the prevailing foliation; a few grains, however, define another foliation that forms a large angle to the major foliation. Quartz grains are divided into sub-grains, but the sub-grain texture is much less pronounced than in the other two samples. Feldspars are better preserved than in the two other samples.

Experimental techniques

Polished petrographic thin sections were prepared using a wax soluble in alcohol. Three of these thin sections were selected for chemical analysis with a Jeol JSM 6400 Scanning Electron Microscope equipped with an EDS spectrometer. Areas of interest for TEM study were selected from the same specimens and mounted on 3 mm diameter copper grids. Electron transparent films were prepared by removing the specimens with the Cu mounts from the thin sections and subsequent thinning by accelerated argon ions in an Ion Tech mill. The specimens were lightly coated with carbon. TEM investigations were carried out with a Jeol 2000FX microscope operating at 200 keV (*Ferrow* and *Ripa*, 1990).

Experimental results and discussion

Optical microscopy, X-ray diffraction, and microprobe analyses

Five thin sections were studied with optical and electron microscopy. The mineral assemblages of these samples are largely similar (Fig. 2) but differ in terms of

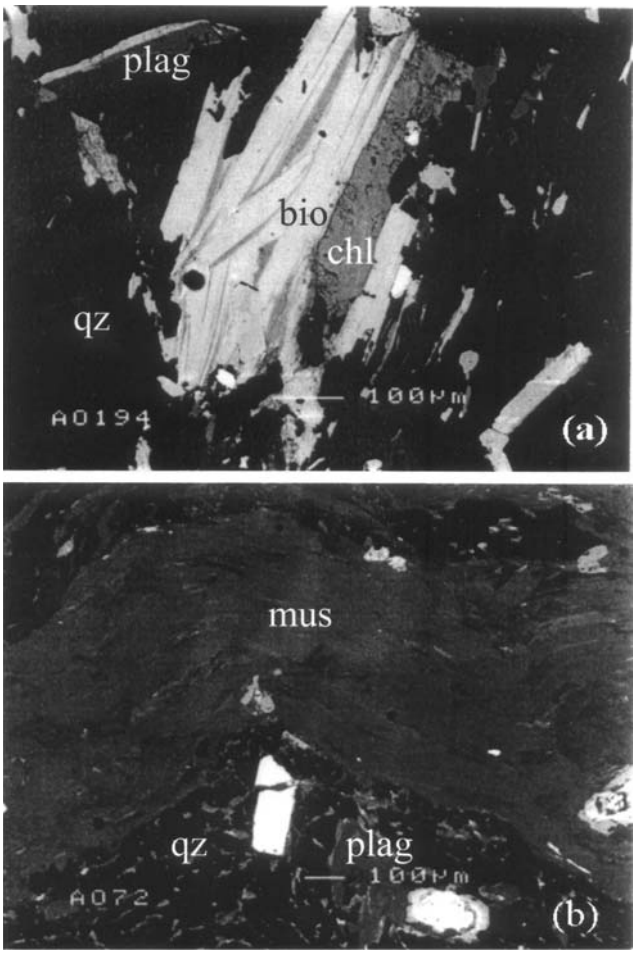

Fig. 2. Electron micrograph of the mylonite samples S194 and S72 showing the major phases (**a**) and the degree of deformation (**b**)

deformation state. Samples S72 and S371, for example, both show well developed shear bands although the deformation is more pronounced in sample S72 (Fig. 2b). Recrystallization and the occurrence of undulatory extinction in quartz porphyroclasts and neoblasts, as well as the occurrence of exsolution lamellae in plagioclase feldspar, are all features that developed during mylonitization. The amount of recrystallization increases with increasing deformation. For example, the fine-grained biotites occur in the most intensely deformed parts, and the amount of muscovite is more abundant in areas that have suffered intense deformation. Biotite is in contact with muscovite and chlorite, suggesting that its formation is related to the presence of muscovite and chlorite.

The main minerals are, in decreasing abundance, quartz, plagioclase, muscovite, chlorite, and biotite (Fig. 2). Accessory minerals include apatite, calcite, and ilmenite. The grains are homogeneously distributed. The quartz grains show undulatory extinction and appear as porphyroclasts with sub-angular shapes as well as neoblasts with sub-rounded shapes. The large plagioclase porphyroclasts have a sub-angular shape and show twinning. Very rarely plagioclase neoblasts have been observed. The mica grains are often in contact with plagioclase and quartz grains

Table 1. *Microprobe analyses of the micas, chlorite and plagioclase. The chemical formulae were calculated based on 22 oxygens for biotite and muscovite, 28 oxygens for chlorite, and 8 oxygens for plagioclase*

Sample S	Biotite 194	Biotite 371	Muscovite 371	Muscovite 72	Chlorite 194	Chlorite 72	Plagioclase 371
SiO_2	37.1	36.8	46.6	46.9	26.9	27.8	63.7
Al_2O_3	15.3	16.6	31.2	30.6	17.3	17.0	22.9
FeO	21.2	18.7	4.4	4.9	25.8	25.4	0.1
MgO	10.1	11.4	1.3	1.6	15.4	15.5	na
TiO_2	2.3	2.4	1.3	1.1	na	na	na
K_2O	9.8	9.6	9.8	10.6	na	na	0.1
Na_2O	0.2	0.2	0.6	0.5	na	na	9.0
CaO	na	na	na	na	na	na	3.7
Sum	96.0	95.6	95.2	96.2	85.4	85.6	99.5
Si	5.67	5.57	6.31	6.32	5.84	5.98	2.84
$^{[4]}Al$	2.33	2.43	1.69	1.68	2.16	2.02	1.20
$^{[6]}Al$	0.42	0.51	3.28	3.18	2.27	2.30	
Fe^{2+}	2.71	2.37	0.50	0.55	4.69	4.58	
Mg	2.30	2.57	0.26	0.32	4.99	4.99	
Ti	0.53	0.27	0.13	0.11			
K	1.91	1.85	1.69	1.82			0.01
Na	0.06	0.06	0.11	0.13			0.77
Ca							0.18

na not analysed

and have elongated and flattened shapes parallel to the shear bands. They are more flattened in areas where the shear bands are well developed. In S194, less deformed than the other samples, several intergrowths of biotite grains are observed.

Microprobe analyses of micas and plagioclases from three samples are presented in Table 1. The chemical formulae were calculated based on 22 oxygens for biotite and muscovite, 28 oxygens for chlorite, and 8 oxygens for plagioclase. Overall compositions of the biotite, muscovite, chlorite and plagioclase from the different localities are similar. The biotites are rich in Al, the muscovites are 'phengitic' in composition, and the feldspars are sodic plagioclase.

Cipriani et al. (1971) and *Thompson* (1974) have shown that the paragonite content in muscovite varies with temperature, and that $Na/(Na + K)$ first increases with increasing temperature, reaching a maximum value of 0.35 at $\sim$550 °C, and then falling as temperature continues to rise. The paragonite content is low, which according to *Cipriani* et al. (1971) and *Thompson* (1974) would indicate either a low or a high metamorphic temperature. Considering that the specimens come from mylonitic rocks, it is most likely that low $Na/(Na + K)$ is indicative of high temperature metamorphism, i.e. higher than 500 °C. Additional information on the temperature of formation of these rocks is obtained by calculating the K_d values for 'phengite' and chlorite pairs. The K_d value for one 'phengite'/chlorite pair in Table1 is 1.86, indicating a metamorphic temperature higher than 400 °C

(*Sillanpää*, 1986) and confirming that the low $Na/(Na + K)$ in muscovite is indeed an indicator of high temperature metamorphism.

Sassi and *Scolari* (1974) and *Sassi* et al. (1976) have shown that the 'phengite' content of muscovite may be used to estimate the pressure of metamorphism. *Cipriani* et al. (1971), *Frey* et al. (1983), and *Sillanpää* (1986) were able to correlate the length of the observed b-axis, b_0, of 'phengitic' muscovite, calculated from x-ray powder diffraction data, with its Fe and Mg content, obtained by microprobe analysis. It is therefore possible to estimate metamorphic pressure for pelitic bulk compositions directly from x-ray diffraction data. These observations render the 'phengite' content in muscovite a very useful petrogenetic indicator.

However, bulk rock chemistry and fluid composition are known to have some influence as well (*Sillanpää*, 1986). *Ferrow* et al. (1990) have shown that 'phengite' is not a single phase but comprises fine intergrowths of celadonite exsolutions in muscovite. Selected area electron diffraction (SAED) of 'phengites' from this study show splitting of the (00l) reflections, similar to that reported by *Ferrow* et al. (1990). These 'phengite' phases are, therefore, composed of a pure muscovite host and fine exsolutions of celadonite, increasing the number of phases in the system by one. Nonetheless, the observation does not undermine the findings of *Cipriani* et al. (1971), *Thompson* (1974), and *Sillanpää* (1986) since the host muscovite in 'phengite' is passive during metamorphic reactions of pelitic rocks. For example, the appearance of the biotite isograd in true pelites can be written as

$$\text{celadonite} + \text{chlorite} \rightarrow \text{biotite} + \text{muscovite} + \text{quartz} + H_2O \qquad (1)$$

where only the celadonite content of 'phengite' is involved in the reaction.

Similarly, the change in b_0-value in 'phengite' reflects the change in its celdonite content since for a pure phase the b_0 of muscovite is constant. It is, thus, still possible to use the b_0 of phengite to estimate the amount of celadonite exsolution and use the information obtained to estimate the pressure of pelitic rocks. The term phengite, written without quotation marks, will henceforward be used to indicate an ideal muscovite host with fine exsolutions of celadonite, with all Fe and Mg attributed to celadonite.

The b_0-values of phengites of the MZ, calculated from the powder x-ray data, are 9.028 (S371) and 9.033 Å (S72), indicating that phengite compositions formed at intermediate to high pressure (*Cipriani* et al., 1971; *Frey* et al., 1983; *Sillanpää*, 1986). Consequently, the mylonite rocks in the MZ were metamorphosed at intermediate to high pressure and at temperatures $\geq 500\,^{\circ}C$.

Pressure and temperature are not the only parameters controlling the phengite composition. The bulk composition of the rock, the degree of oxidation, and partial water pressure are also known to influence the composition of metamorphic phengites (*Guidotti* and *Sassi*, 1976). For example, if the protolith is poor in Al_2O_3 and rich in FeO and MgO, then biotite will be a stable phase in the early stage of metamorphism. The b_0 values of phengites will then be large, seemingly indicative of high pressure metamorphism (*Sillanpää*, 1986). The b_0 value, taken on its own, thus gives insufficient information to estimate pressure conditions. Note, however, that the rocks in this study, similar to those studied by *Sillanpää* (1986), are rich in Al_2O_3 and indicate that phengite was formed at pressures ranging between 0.3 and 0.4 GPa.

Electron microscopy

Microprobe analyses (Table 1) show that plagioclase is poor in calcium. The anorthite content is 1.1 mole % and plots within the peristerite range. The major and minor phases in the peristerite were approximately 59 and 12 nm in width, respectively, and the interfaces appear sharp in the TEM micrographs (Fig. 3). Note also that the exsolution is quite periodic. The chemical composition of the minor phase was not measured in this study although *Cliff* et al. (1976) using analytical electron microscopy, and *Brown* (1969) using X-ray diffraction, have estimated the composition of the minor phase to be An_{21-30}.

The metamorphic biotite grains in mylonite rocks from the MZ contain one distinct type of defect structure, i.e. straight micro-cavities parallel to (001) (Fig. 4). Unlike observations made by *Bell* et al. (1986), all micro-cavities observed in this study are straight. Moreover, they have limited extent, and they are not associated with kink bands as micro-cavities usually are. These cavities are potential channels for transport of fluids and serve as sites for brucitization of the biotite interlayer (*Banos* et al., 1983). The chlorite layers included within the biotite grains in Fig. 2a could be formed by retrograde brucitization of biotite along these micro-cavities.

The diffraction pattern in Fig. 4 shows that the biotite is a 2M polytype. The absence of streaking along c^* indicates that stacking faults are absent. It is difficult

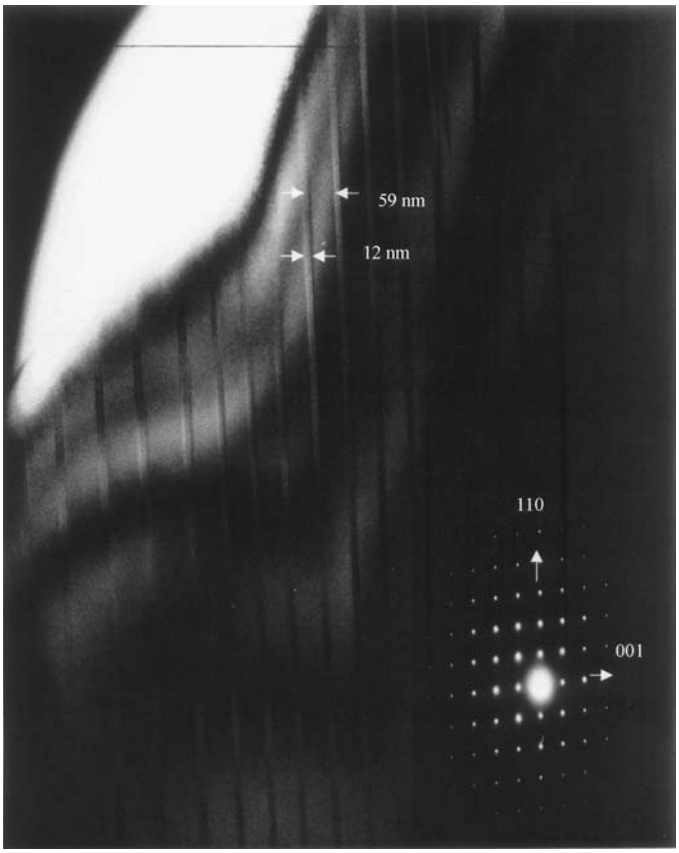

Fig. 3. A 'peristerite' microtexture showing intergrown, nanometer-sized albite and oligoclase lamellae. The major and minor phases in the peristerite are approximately 59 and 12 nm in width, respectively, and the interfaces between them appear sharp in the TEM micrographs. Note also that the exsolution is quite periodic

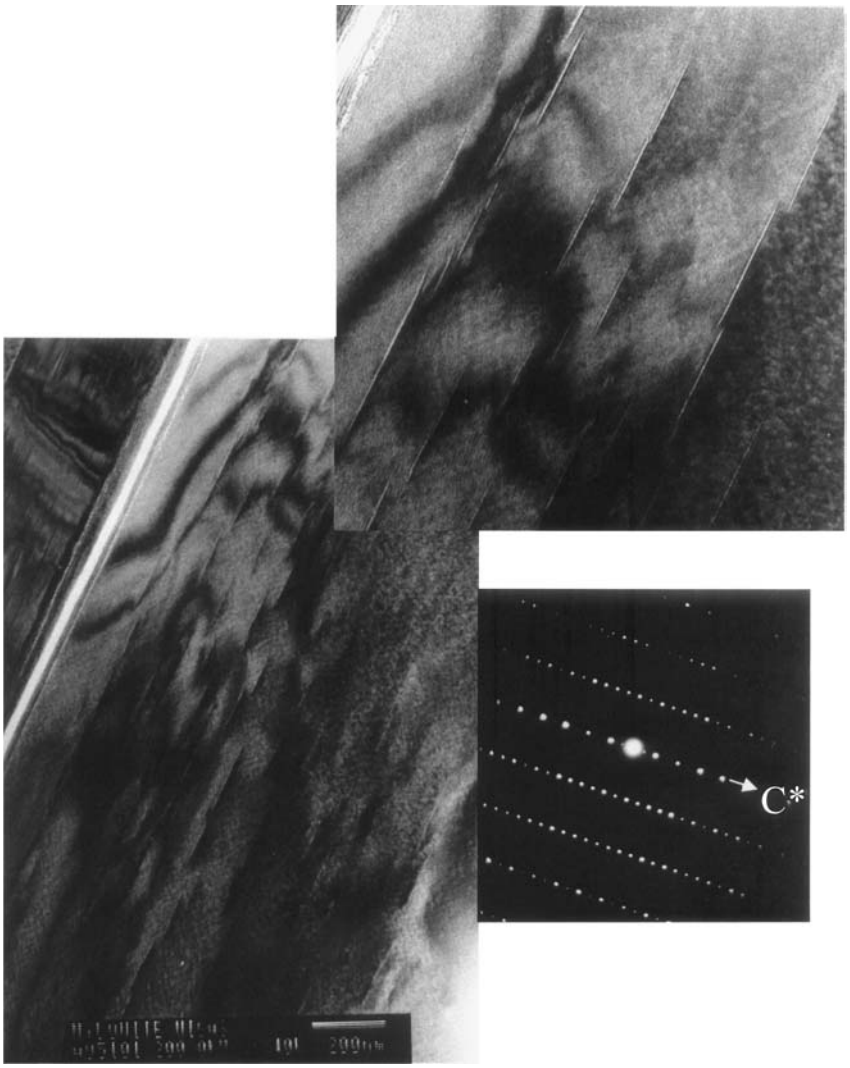

Fig. 4. Bright-field conventional TEM micrograph of biotite showing straight microcavities (inset). The SAED shows that the sample is a 2M polytype

to estimate the dislocation distribution in the biotite grains because of the relatively small area examined by TEM. Nonetheless, both regions with high and low dislocation density are observed although in general most of the grains studied have low dislocation densities. The dislocations perturb the biotite layering (Fig. 5). In addition to dislocation faults, low-angle grain boundary is another defect that is often observed in biotite.

The most common polytype in biotite is the one-layer polytype (*Bailey*, 1984) although multi-layer polytype structures are also observed (*Bell* and *Wilson*, 1977, 1981). The number of stacking faults and their way of ordering determines the polytype structure. The most common multi-layer polytype structure in these biotites is the $2M_1$, but a 10 layers polytype is also observed (Fig. 6).

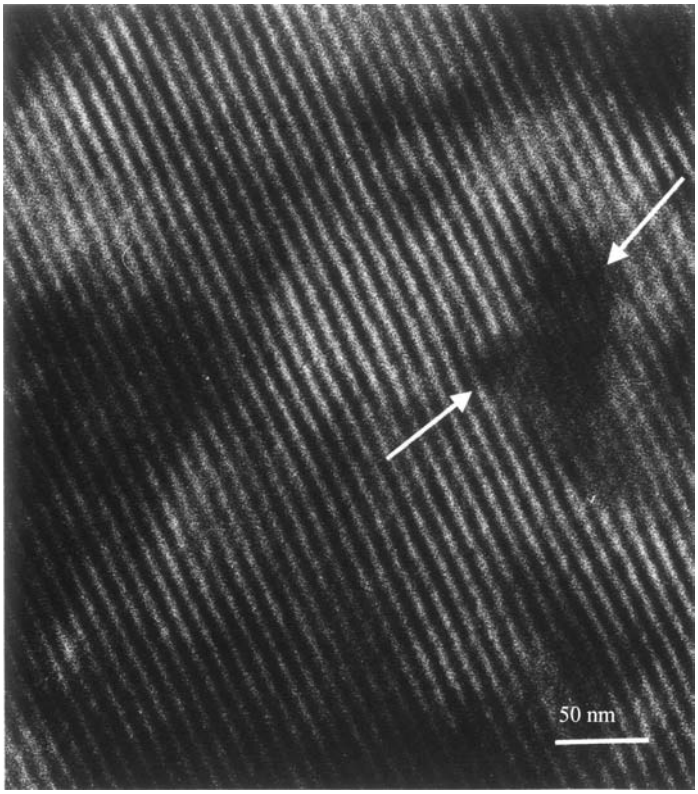

Fig. 5. High-resolution TEM image of biotite showing disruption of the layering by dislocation

According to *Bell* and *Wilson* (1977), stacking faults and polytypes are strongly related to each other. Under applied stress, deformation and shearing causes the development of dislocations. Most of the dislocations observed are dissociated into partial dislocations because of the low stacking fault energy in biotite. These stacking faults can develop into either a stacking order or a stacking disorder. The diffraction patterns in Fig. 5 indicate that the stacking faults created an ordered $2M_1$ polytype structure, a polytype very common in slightly deformed biotite grains with a low dislocation density (*Bell* and *Wilson*, 1981). In more deformed biotites, however, the dislocation density and the density of stacking faults increase with increasing strain while the spatial ordering of stacking faults decreases.

In this case, the occurrence of a $10M_1$ polytype structure provides further evidence for low strain during deformation of these rocks, suggesting a high degree of order of stacking faults. In such biotites, superlattice structures are quite common. Spatial disordering is also found in biotites and chlorites from the rocks of the MZ, as shown by the presence of streaking in their diffraction patterns (Fig. 7).

Streaking occurs if there is a high density of stacking faults. A high density of stacking faults indicates that high strains were achieved (*Bell* and *Wilson*, 1981). The degree of streaking or stacking disorder is more pronounced for the chlorite than for the biotite because the diffraction pattern of chlorite does not show clear

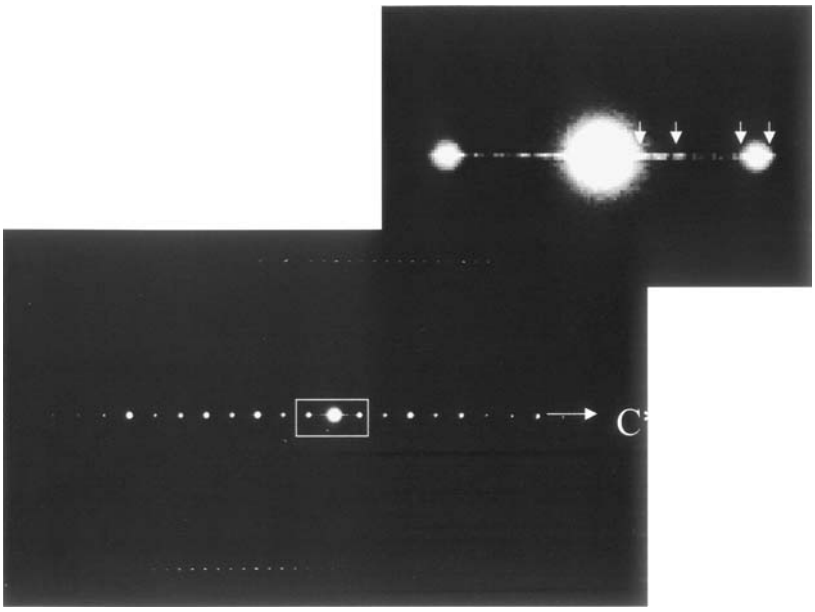

Fig. 6. SAED of multi-layered biotite polytype. The insert shows diffraction spots between (000) and (001), indicating a 10M polytype

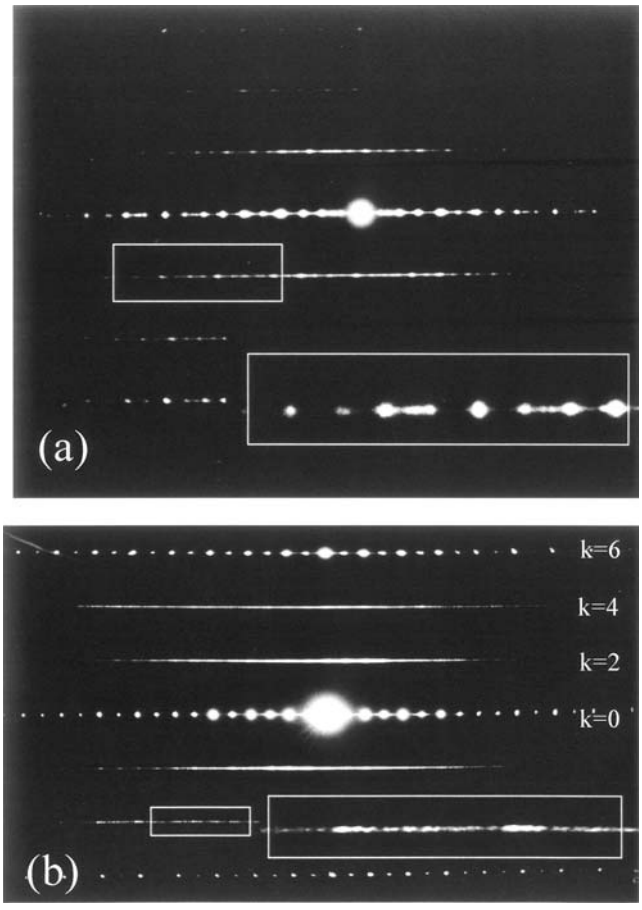

Fig. 7. SAED of biotite (**a**) and chlorite (**b**) with stacking faults. The inserts in the lower right are magnified images of the rectangles shown in each micrograph

superlattice reflections in the $k = 2$ and $k = 4$ rows (Fig. 7b), while in the same row the diffraction pattern of biotite has super lattice reflections, although they are only weakly streaked (Fig. 7a). The degree of streaking is an indication of the intensity of deformation. Accordingly, the biotite grains are less deformed than the chlorite grains. Note, however, that the inserts in Fig. 7 show that the streaking in biotite is weak and that the streaking in chlorite, where $k = 4$, is discontinuous.

The TEM observations of the low-angle grain boundary indicate that grain size reduction processes were active. During this later stage of deformation, the deformed biotite grains become reduced in size by the formation of biotite neoblasts. This grain-size reduction process continues and the dislocations start to rearrange into a low-angle grain boundary by glide. The re-arrangements of these dislocations cause a spatial order of stacking faults that is shown in the diffraction pattern, resulting in a $2M_1$ polytype structure.

High-resolution TEM images show chlorite lamellae within the biotite structure (Fig. 8). Mylonitization is a progressive form of metamorphism where low-grade minerals such as chlorite are consumed and higher-grade minerals like biotite are stabilized (cf. eqn. 1). The presence of chlorite in biotite indicates that these textures are retrograde relative to mylonitization, and possibly formed by brucitization along the micro-cavities imaged in Fig. 4.

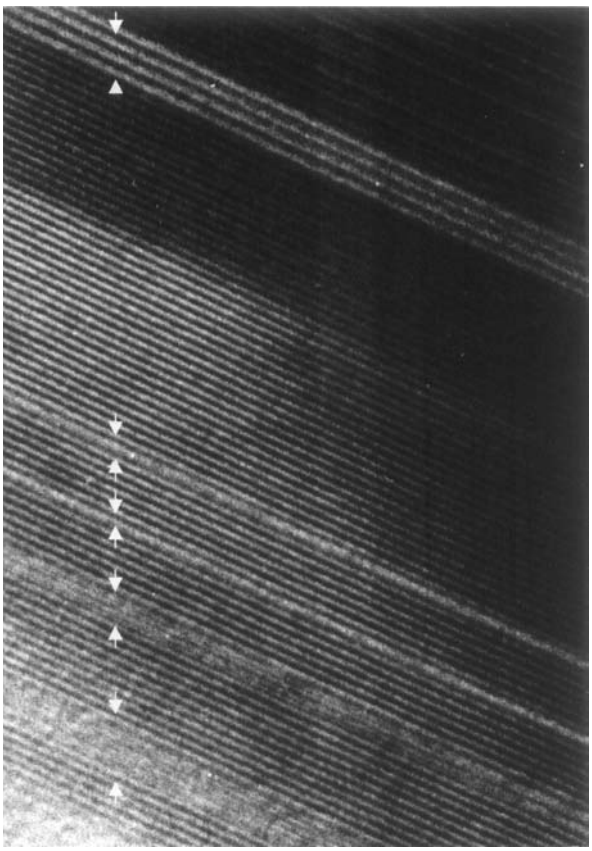

Fig. 8. High-resolution TEM image of biotite intergrown with chlorite (arrows); chlorite probably formed by brucitization along the micro-cavities shown in Fig. 4. Two consecutive dark fringes in biotite are 1 nm apart

Conclusions

Several different chemical substitution reactions occurred during deformation of the granitic mylonites. The phengite, paragonite and Mg-Fe^{2+} distribution between muscovite and chlorite are used as geobarometer and geothermometers, respectively. They all indicate that deformation took place in a pressure range of 0.3 to 0.4 GPa at a relatively high temperature of $\geq 500\,^{\circ}C$.

The intensity of deformation was not identical in the granitic mylonites. There are areas where the rock is highly deformed, indicated by the appearance of well-developed shear bands, recrystallized quartz grains, undulatory extinction in both quartz porphyroclasts and neoblasts, and exsolution lamellae in plagioclase. Other areas are less deformed.

The occurrence of dislocations and low-angle grain boundaries, formed by the re-arrangement of these dislocations during grain-size reduction processes, confirms that the rock is deformed. The deformation occurred at low temperature. The rate of deformation is controlled by the glide of dislocations.

Stacking order and disorder can be used as strain indicators. Biotites that formed during low strain conditions show a high degree of spatial stacking ordering. Biotites and chlorites that formed under high strain conditions show a high degree of spatial stacking disorder. The occurrence of both ordered and disordered stacking faults indicates that the intensity of deformation was not uniform through the entire MZ.

The occurrence of chlorite domains within biotite is probably related to retrograde brucitization, along micro-cavities that formed parallel to (001) during mylonitization. Chlorite flakes not associated with biotite are most likely primary in origin.

Acknowledgments

The project was funded by financial support to *E. Ferrow* and *A. Lindh* by the Swedish Research Council, NFR. *A. Ooteman*'s stay in Lund, Sweden, was made possible by the Erasmus student exchange program. The paper benefitted from reviews by *F. Brenker* and *R. Yund*.

References

Bailey SW (1984) Classification and structures of the micas. In: *Bailey SW* (ed) Rev Mineral 13: 1–12

Banos JO, Amouric M, Fouquet CD, Baronnet A (1983) Interlayering and interlayer slip in biotite as seen by HRTEM. Am Mineral 68: 754–758

Bell IA, *Wilson CJL* (1977) Growth defects in metamorphic biotite. Phys Chem Minerals 2: 153–169

Bell IA, *Wilson CJL* (1981) Deformation of biotite and muscovite; TEM microstructure and deformation model. Tectonophysics 78: 201–228

Bell IA, *Wilson CJL, Mclaren AC, Etheridge MA* (1986) Kinks in micas: role of dislocations and (001) cleavage. Tectonophysics 127: 49–65

Brown WL (1969) X-ray studies in the plagioclases, part 2. The crystallographic and petrologic significance of peristerite unmixing in the acid plagioclase. Z Kristallogr 113: 297–344

Carreras J, Cobbold PR, Ramsay JG, White S (1980) Shear zones in rocks. J Struct Geol 2: 119–126

Cipriani C, Sassi FP, Scolari A (1971) Metamorphic white micas: definition of paragenetic fields. Schweiz Mineral Petrogr Mitt 51: 259–302

Cliff G, Champness PE, Nissen HU, Lorimer GW (1976) Analytical electron microscopy of exsolution lamellae in plagioclase feldspars. In: *Wenk HR* (ed) Electron Microsc in Minerals: 258–265

Ferrow EA, Ripa M (1990) Al-poor and Al-rich orthoamphiboles: a Mössbauer spectroscopy and TEM study. Mineral Mag 54: 547–552

Ferrow EA, London D, Goodman KS, Veblen DR (1990) Sheet silicates of the Lawler Peak granite, Arizona: chemistry, structural variations and exsolution. Contrib Mineral Petrol 105: 491–501

Frey M, Hunziker JC, Jaeger E, Stern WB (1983) Regional distribution of white K-mica polymorphs and their phengite content in the Central Alps. Contrib Mineral Petrol 83: 185–197

Guidotti CV, Sassi FP (1976) Muscovite as a petrogenetic indicator mineral in pelitic schists. N Jb Mineral Abh 127: 97–142

Lindh A (1974) The Mylonite Zone in south-western Sweden (Värmland): a re-interpretation. Geol Fören Stockh Förh 96: 183–197

Lindh A (1980a) Correlation of Landsat lineaments in the south-western margin of the Baltic Shield. Geol Fören Stockh Förh 102: 1–12

Lindh A (1980b) Some observations on white micas in a shear zone. N J Mineral Abh 138: 165–177

Lindh A (1998) Beskrivningar av berggrunden i västra delen av Värmlands län med undantag för Gillbergaskålen (in Swedish with an English summary). In: *Ek A* (ed) Beskrivning till Berggrundskartan över Värmlands län Västra Värmlands berggrund. Sverig Geol Unders Ba 45: 3–267

Lundegårdh PH, Lindh A, Gorbatschev R (1992) Berggrundskarta över Värmlands län (Map of Bedrock geology of Värmland County). Sverig Geol Unders Ba 45

Page L, Möller C, Johansson L (1996) $^{40}Ar/^{39}Ar$ geochronology across the Mylonite Zone and the southwestern granulite province in the Sveconorwegian orogen of S Sweden. Precamb Res 79: 239–259

Sassi FP, Scolari A (1974) The b_0 value of the potassic white micas as a barometric indicator in low-grade metamorphism of pelitic rocks. Contrib Mineral Petrol 45: 143–152

Sassi FP, Kräutner HG, Zirpoli G (1976) Recognition of the pressure character in greenschist facies metamorphism. Schweiz Mineral Petrogr Mitt 56: 427–434

Sillanpää J (1986) Mineral chemistry study of progressive metamorphism in calcareous schists from Ankavattnet, Swedish Caledonides. Lithos 19: 141–152

Thompson AB (1974) Calculation of muscovite-paragonite-alkali feldspar phase relations. Contrib Mineral Petrol 44: 173–194

Authors' address: *E. A. Ferrow* (corresponding author; e-mail: embaie.ferrow@geol.lu.se), *A. Ooteman* and *A. Lindh*, Department of Geology, Lund University, Sölvegatan 13, SE-223 62 Lund, Sweden